

# Properties and Microstructures of Rapidly Solidified Zirconia-Based Ceramic Alloys

R. P. INGEL, D. LEWIS, III, AND B. A. BENDER

U.S. Naval Research Laboratory  
Ceramics Branch  
Washington, DC 20375

S. C. SEMKEN

Massachusetts Institute of Technology  
Department of Materials Science and Engineering  
Cambridge, MA 02139

Rapid solidification of molten ceramic alloys is a disequilibrium process retaining metastable solid assemblages and fine microstructures, with potential for improved properties in the resultant product. In zirconia-based alloys, rapid solidification stabilizes the high-temperature tetragonal  $\text{ZrO}_2$  phase by kinetic means in uniformly fine structures. The unique character of the phases and microstructures formed offers insight into the development of equilibrium and disequilibrium assemblages in zirconia systems. We have rapidly quenched several zirconia-based alloy melts by various techniques at different rates, to study kinetic stabilization of tetragonal  $\text{ZrO}_2$  and development of metastable phases and microstructures. XRD, SEM, TEM, and Raman spectroscopy of these rapidly solidified alloys indicate relationships among cooling rate, composition, and structure considerably different from those in more slowly cooled ceramics. The results indicate that, at presently attainable cooling rates, diffusive and displacive transformations compete during solidification, subsolidus phase transformations may alter rapidly solidified assemblages, and quenching kinetics alone will not fully stabilize the tetragonal polymorph.

**R**apid solidification is a disequilibrium process enabling retention of metastable phases and fine microstructures. Rapid quenching inhibits diffusion, and thus prevents the formation of the equilibrium crystalline phases and coarser microstructures characteristic of materials cooled more slowly. Rapid solidification techniques range from melt atomization or spinning, with cooling rates of approximately  $10^3$  to  $10^5$  K/s,<sup>1</sup> to splat cooling, with rates on the order of  $10^5$  to  $10^7$  K/s.<sup>2</sup> The unusual microstructures and metastable phases in materials produced by these techniques afford the potential for significant improvement of properties over those of "conventional" materials.<sup>3-7</sup> Although rapid solidification processing (RSP) has been used in metallurgy for many years,<sup>8</sup> it has only recently been applied to ceramics.<sup>9</sup> Ideally, RSP of ceramics should yield microstructures and properties analogous to those of rapidly solidified metals,

such as finer grain size, chemical homogeneity, extended solid solubility, and, with extremely fast cooling, complete amorphism. However, the high liquidus temperatures of ceramic systems make them difficult to melt and to contain without contamination. Their low thermal conductivities, which inhibit the removal of heat, limit cooling rates and usually cause destructive thermal shock in the solid product. Many ceramic alloys are also susceptible to wide variations in stoichiometry at high temperature. As a rule, the technology required to obtain both understanding and control of RSP in ceramic alloy systems, particularly on an experimental scale larger than a few milligrams, has been difficult to achieve.

The rapid solidification of zirconia-based eutectic alloys has been shown<sup>10-15</sup> to stabilize the high-temperature tetragonal  $\text{ZrO}_2$  phase by kinetic means, in a uniformly fine microstructure. This affords the potential for improved mechanical properties through transformation toughening.<sup>16-18</sup> The unique character of the compositions, phases, and structures obtained by RSP also offers insight into stable and metastable phase transformations in zirconia systems. For example, Kalonji et al.,<sup>12</sup> expanding on the work of Boettinger and coworkers,<sup>19,20</sup> used solidification theory to predict microstructures in the rapidly solidified  $\text{Al}_2\text{O}_3\text{-ZrO}_2$  eutectic as a function of composition and cooling rate.

This report describes the phases and microstructures formed in several rapidly solidified zirconia-based ceramic alloys. Subsolidus phase transformations in these metastable materials, and the relative effectiveness of diffusionless quenching and aliovalent-oxide doping in stabilizing tetragonal  $\text{ZrO}_2$ , are also discussed.

## Experimental Approach

We have rapidly solidified zirconia alloy compositions on fixed and moving substrates, by laser-melt quenching and by plasma spraying, to obtain a wide range of cooling rates. Several combinations of zirconia with other oxides: the  $\text{Al}_2\text{O}_3\text{-ZrO}_2$  eutectic, and binary solid solutions of  $\text{ZrO}_2$  with  $\text{Y}_2\text{O}_3$ ,  $\text{CeO}_2$ , and  $\text{TiO}_2$ , were chosen in order to evaluate the influence of various stabilizers on RSP phases and microstructures. X-ray diffraction (XRD), SEM, TEM, and Raman spectroscopy analyses were used to identify and characterize the phases and structures formed in the rapidly-solidified specimens.

## Results and Discussion

### $\text{Al}_2\text{O}_3\text{-ZrO}_2$ Eutectic

An alumina-zirconia eutectic composition (57 wt%  $\text{Al}_2\text{O}_3\text{-43 wt% ZrO}_2$ ) was rapidly quenched from a superliquidus temperature of 2000°C, as a thin layer on rotating and fixed room-temperature substrates. The cooling rate on the fixed substrate has been approximated as  $10^2$  to  $10^3$  K/s, while for the rotating substrate the cooling rate was roughly  $10^4\text{-}10^5$  K/s. Increased cooling rate produced eutectic structures of similar morphology but of decreasing lamellar spacing<sup>14,15</sup> with the finest spacing being approximately 20 nm. Scanning electron microscopy (SEM) of the material showed the grain sizes to be approximately 10 to 100  $\mu\text{m}$ , ranging from equiaxed to columnar in shape.<sup>15</sup> X-ray diffraction and transmission electron microscopy (TEM) indicated that 80 to 95 vol% of the  $\text{ZrO}_2$  was retained as tetragonal, a higher fraction than in conventionally processed ceramic alloys.<sup>15</sup> A dendritic structure, found at the center of each grain, has been identified as an  $\text{Al}_2\text{O}_3$ -rich phase<sup>13,15</sup> and relates to the initial nucleation site of the grain. A very fine lamellar eutectic microstructure was observed in the central regions of the grains; this coarsened toward the grain boundaries. The coarsening arises as a

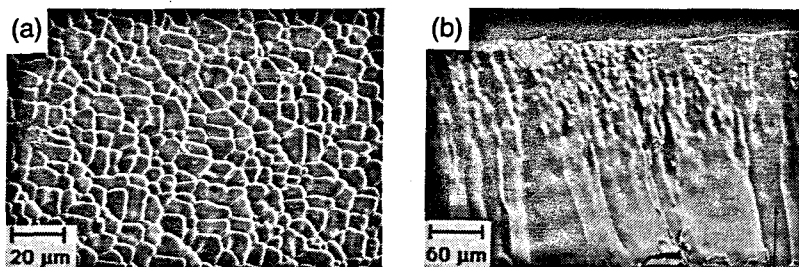


Fig. 1. Scanning electron micrograph of a rapidly solidified 8 wt%  $\text{Y}_2\text{O}_3$  zirconia alloy. (a) The external radiative cooled surface with very fine uniform grains; (b) cross section of the solidified specimen with the arrow indicating the general solidification direction.

result of intragrain variations in the cooling rate and composition.<sup>12</sup> Between the zirconia lamellas, a precipitate-free zone of pure alumina was observed, and then a central area having a very fine mottled structure. This mottled structure arises from the precipitation of very fine zirconia particles during the latter stages of solidification. The study of the eutectic structure has been instructive in examining the variations in microstructure associated with cooling rates obtained by different rapid solidification processes.

#### $\text{ZrO}_2\text{-Y}_2\text{O}_3$

Zirconia alloyed with 8 wt%  $\text{Y}_2\text{O}_3$  (8-YSZ) was rapidly solidified as a thin layer on room-temperature substrates. Figure 1(a) is an SEM photo of the external surface of a thin solidified layer, showing a uniform distribution of fine grains on the order of 5 to 10  $\mu\text{m}$  in size. A cross section of the specimen (Fig. 1(b)) reveals that solidification began at the melt-substrate interface (bottom of photo), immediately retarding downward heat transfer and allowing the nucleation and growth of comparatively large grains, approximately 65 to 100  $\mu\text{m}$  in diameter. The thin layer of extremely fine grains at the opposite (upper) surface is indicative of fast radiative and convective (air) cooling. The center of the specimen solidified as columnar grains, parallel to the upward removal of heat, with the acceleration of the solidification rate reflected by the formation of finer grains and entrapped pores.

X-ray diffraction and Raman spectroscopy showed that all of the  $\text{ZrO}_2$  was retained as tetragonal. The microstructure of this material was similar to that in other yttria-zirconia alloys rapidly quenched by different techniques<sup>21</sup>; it exhibited structures characteristic of the metastable tetragonal phase identified as  $t'$  by previous investigators.<sup>22-24</sup> Figure 2(a) and (b) are TEM micrographs of a region near the substrate interface, which show the  $t'$  structure of lathlike variants, and wavy fringes that exhibit contrast characteristic of antiphase boundaries (APBs).<sup>25</sup> APBs and variants have been described in other zirconia alloys with different heat treatments.<sup>23,24,26-29</sup> Heuer and Rühle<sup>29</sup> initially attributed the formation of APBs to a composition-invariant cubic  $\rightarrow$  tetragonal massive transformation. However, they believe the displacive transformation is better described as a first-order reaction involving homogeneous nucleation.<sup>30</sup> A "foam" structure<sup>21</sup> was also observed, associated with the APBs occurring within the variants (Fig. 2(a)). This

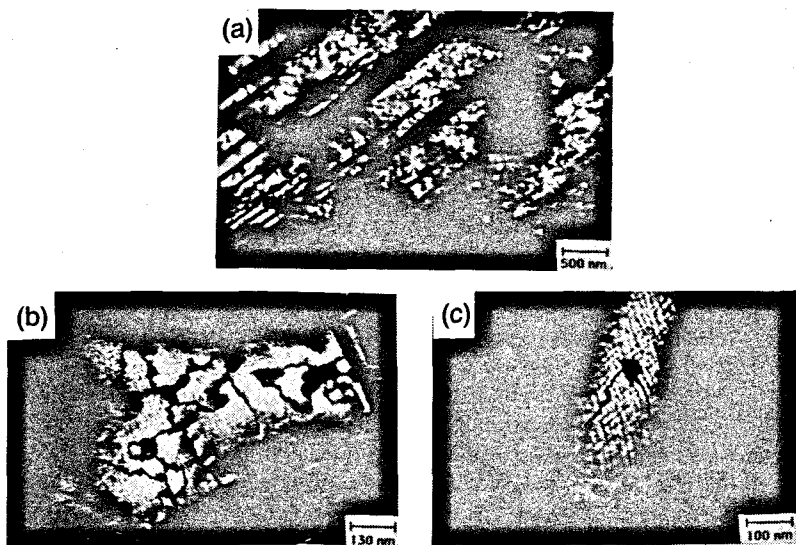


Fig. 2. Transmission electron dark-field micrographs of the rapidly solidified 8 wt%  $\text{Y}_2\text{O}_3$  zirconia shown in Fig. 1. (a) and (b) show the tetragonal variants and the antiphase boundaries with the foam structure; (c) is a higher magnification of a tetragonal variant showing a very fine modulated structure.

has been attributed to ordering phenomena, and has been seen in metallic compounds such as  $\text{Ni}_4\text{Mo}$  (Ref. 31) which, on ordering, transforms from FCC to a distorted tetragonal structure. A very fine modulated or tweed structure occurs within the "foam" (Fig. 2(c)). This may be the precursor of ordering or a diffusion-controlled phase transformation.

The metastable tetragonal phase manifests itself in other morphologies apparently different from those described above. Within several grains of the rapidly solidified 8-YSZ alloy, lenticular plates were found which appeared very similar to plates observed by Sakuma et al.<sup>32</sup> and Anderson et al.<sup>33,34</sup> in more slowly cooled alloys. They found these to be tetragonal plates growing into a cubic matrix. However, in the present rapidly solidified alloy, these structures were found to be growing into a tetragonal matrix, as confirmed by SAED. SAED within the matrix between the tetragonal plates at the same orientations as the plates showed no extra reflections which would suggest that the matrix was cubic  $\text{ZrO}_2$ . However, tilting of the foil to different orientations of the matrix revealed nonallowed cubic reflections, verifying that the matrix was tetragonal  $\text{ZrO}_2$ . Our observations concur with those of Lanteri et al.,<sup>24</sup> who postulated that the displacive cubic  $\rightarrow t'$  transformation always goes to completion in yttria-zirconia alloys in this composition range. These same investigators also noted<sup>24</sup> that the lenticular tetragonal plates occur with greatest frequency in polycrystalline alloys, suggesting that they are mechanical accommodation twins.

Within other grains of this same RSP material, variants were observed with a coarser tweed structure than that shown in Fig. 2(c). This tweed structure

consists of alternating light and dark lamellas. This modulated structure was also observed by Sakuma et al.<sup>32,35,36</sup> in image arc melt-grown single crystals of yttria-zirconia subjected to various heat treatments. Their electron diffraction analyses of this modulated structure in a rapidly solidified 8-YSZ alloy resulted in diffraction patterns with satellites aligned in  $\langle 111 \rangle$  directions. Sakuma et al.<sup>35,36</sup> cited these as evidence of a spinodal decomposition reaction; alternatively, they may indicate a quenched-in early stage of nucleation and growth.<sup>37</sup> We favor the latter explanation, based on the yttria-zirconia phase diagram.<sup>38</sup>

These microstructural variations indicate that different reactions are occurring within the same sample. As noted above, the  $t'$  microstructure indicates that a displacive phase transformation has taken place.<sup>24,29</sup> The presence of the modulated tweed structure is an indication that diffusion-controlled precipitation has also occurred. The fact that microstructures indicative of all of these types of transformations have been observed within one homogeneous alloy composition implies that these various reactions arise as a result of variations in cooling rates, and not necessarily large compositional gradients. Such gradients would be small if the cooling rates were high enough to hinder interdiffusion. Analytical electron microscopy utilizing probe sizes of 20 nm is now being undertaken to determine the magnitude of any compositional variations within the RSP alloys.

The rapidly solidified 8-YSZ alloy was crushed and plasma-sprayed onto a superalloy pin, in order to examine the effects that a subsequent high cooling rate ( $10^5$  to  $10^7$  K/s) RSP technique<sup>39</sup> would have on the initial RSP morphology. This material appeared to be similar in microstructure to similar coatings previously studied,<sup>21,39,40</sup> except that no second-phase inclusions were observed. The microstructure of this plasma-sprayed coating consists of rows of columnar grains typical of plasma-sprayed materials<sup>18,39,40</sup> with no glassy phase present, and also had areas of very fine,  $\approx 100$  nm tetragonal grains. Transmission electron microscopy, Raman spectroscopy, and XRD analyses showed that no monoclinic  $\text{ZrO}_2$  was present. Some microcracking was observed between horizontal bands of the columnar grains, and fine pores of about 20 nm diameter were observed along some grain boundaries as a result of the spraying process. Transmission electron microscopy analyses within the grains (Fig. 3(a)) showed a few tetragonal variants and APBs present throughout the grains (Fig. 3(b)) with SAED confirming that the material was tetragonal ( $t'$ ). The plasma-sprayed RSP alloy did not retain any of the fine tweed structure seen in the starting material or in other rapidly quenched mixed-oxide powders (Fig. 3(c),(d)). The extremely rapid solidification during plasma spraying apparently does not allow this fine structure to form, indicating that this may be the result of diffusional processes.

Other  $\text{Y}_2\text{O}_3$ - $\text{ZrO}_2$  compositions were rapidly quenched onto room-temperature substrates, in the same manner as the 8-YSZ alloy, in order to determine the effects of RSP conditions on the structures and morphologies of lower yttria-stabilizer concentrations. A zirconia alloy rapidly solidified with 5 wt%  $\text{Y}_2\text{O}_3$  was found to have the same structures and phase assemblages as the 8 wt% material. However, for a 4 wt%  $\text{Y}_2\text{O}_3$  composition (4-YSZ), the resultant phases and microstructures in the solid product were markedly different. The material contained both monoclinic and tetragonal  $\text{ZrO}_2$ , as indicated by XRD and electron diffraction. Figure 4(a) shows the typical morphology: areas of tetragonal  $\text{ZrO}_2$  in which variants are faintly visible, colonies of twinned monoclinic, and very large trusslike structures of untwinned monoclinic plates. Microcracks were visible where the monoclinic plates impinge on each other and along monoclinic-tetragonal interfaces. Occasional remnant APBs, evidence of a displacive trans-

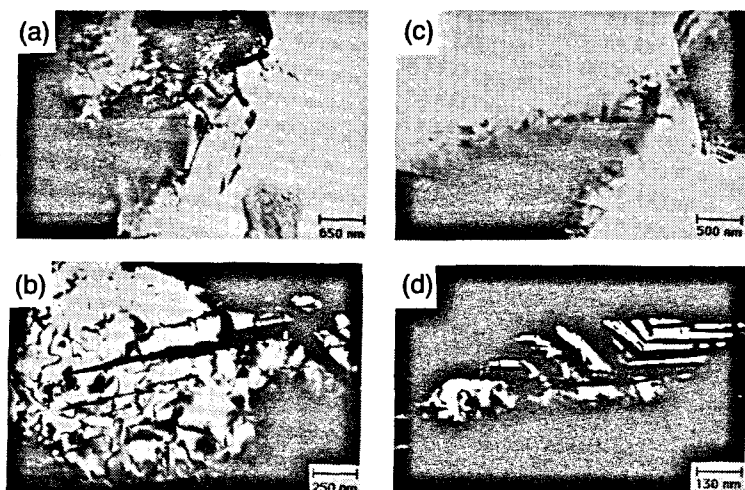


Fig. 3. (a) and (b), TEM micrographs of plasma-sprayed 8 wt%  $\text{Y}_2\text{O}_3$  zirconia RSP material. Note the change in structure from the starting material (Fig. 2) with a subsequent rapid quenching; fewer tetragonal variants and APBs. (c) and (d) Bright-field and dark-field micrographs of rapidly quenched mixed oxide powders show similar structures. However, no fine modulated structure is visible in either of the materials.

formation, were visible within the variants (Fig. 4(c)), but there was no fine tweed structure, as in the higher-yttria content alloys. Between the large monoclinic trusses, the transformation twins have coarsened greatly, as compared to the 8 YSZ alloy, and are internally striated, indicating that strain relief twinning has occurred<sup>41,42</sup> (Fig. 4(b) and 4(d)). Of interest are the unpaired twins which occurred within some tetragonal colonies (Fig. 4(d)). These have also been observed in other rapidly solidified zirconia alloys.<sup>24,44</sup> The unpaired twins and complex twin structures appear to be associated with nonuniform stress states within the specimen, arising from thermal gradients and microcracks between neighboring colonies or grains. Figure 5 shows transformational strain accommodating twin structures in the near region of a microcrack where a portion of the crack is impinging on an adjacent colony. Also this complex twin structure is observed in neighboring colonies and is similar to that which has been identified as a "herringbone" structure by other researchers.<sup>24</sup> However, it appears that these structures arise as a result of accommodation twinning transformations associated with the strains developed during rapid quenching. The dramatic monoclinic trusses may be seen in greater detail in Fig. 6. This is a classic example of autocatalytic martensitic growth<sup>45</sup>; however, the monoclinic plates are not twinned (Fig. 6(b), (c)), but grew in a zig-zag fashion as they impinged on preexisting plates (Fig. 6(c)). The plates are often quite large: 2 to 4  $\mu\text{m}$  long and 0.2 to 0.4  $\mu\text{m}$  wide, with the region between the monoclinic plates being tetragonal  $\text{ZrO}_2$ , as determined by SAED.

In these RSP experiments, the microstructures and phases of the various  $\text{Y}_2\text{O}_3$ - $\text{ZrO}_2$  alloys were sensitive to bulk composition as well as cooling rate.

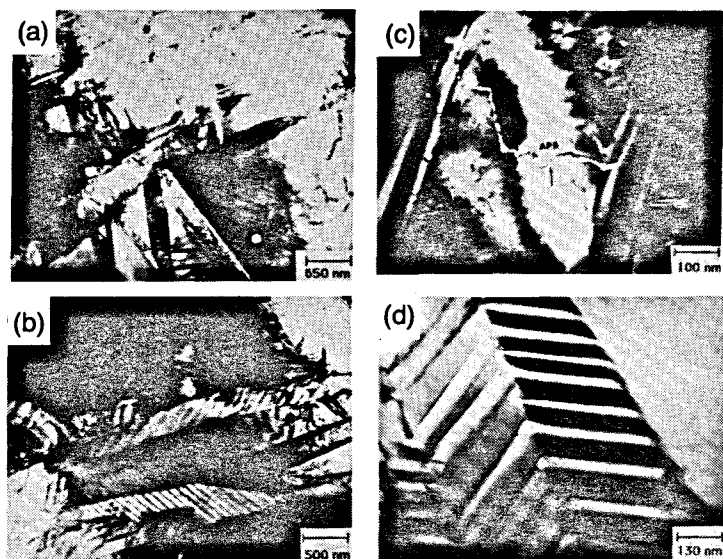


Fig. 4. Transmission electron microscopy bright-field micrograph of a 4 wt%  $Y_2O_3$  RSP alloy. (a) shows that the microstructure is a mixture of tetragonal and monoclinic phases with microcracks at the intersections of the variants and monoclinic plates; (b) colonies of tetragonal variants; (c) (dark-field) remnant APB which extends between and through two tetragonal variants; (d) higher magnification of a tetragonal variant, showing what appears to be unpaired twins. This indicates that a very complex stress state is present.

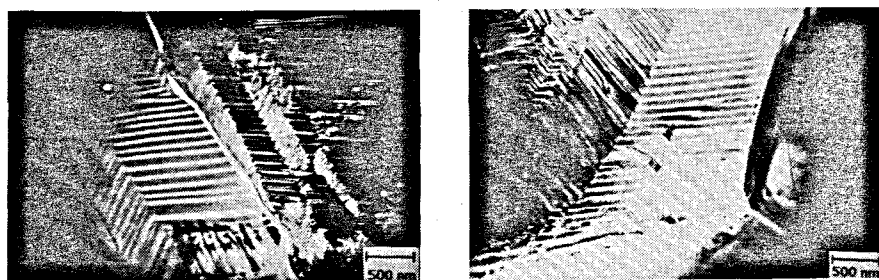


Fig. 5. Transmission electron microscopy bright-field micrographs of accommodation twin structures near a microcrack (left) and in neighboring colonies (right).

Ideally, quenching kinetics should stabilize the high-temperature zirconia polymorphs at any composition. However, given the cooling rates currently attainable, by experiment, an aliovalent-oxide dopant was still necessary for complete stabilization. Scott<sup>22</sup> and Sakuma et al.<sup>32</sup> have also investigated

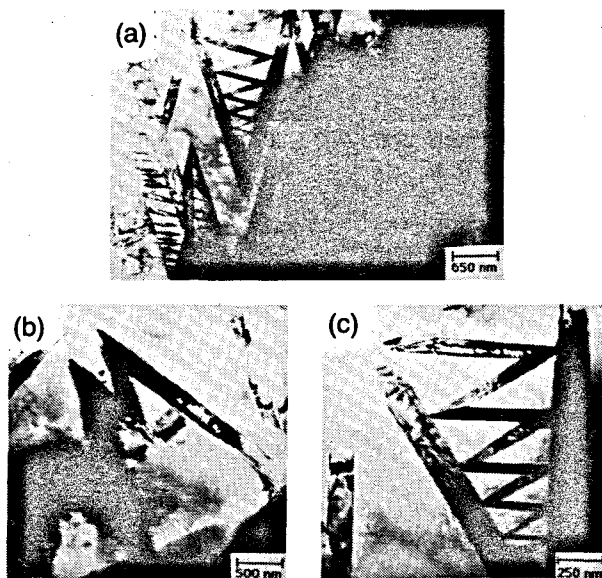


Fig. 6. Transmission electron microscopy bright-field micrographs of the 4 wt%  $\text{Y}_2\text{O}_3$  RSP alloy showing the large monoclinic plate structures found throughout the material: a result of an autocatalytic martensitic transformation. The matrix between the monoclinic plates was found by SAED to be tetragonal.

yttria-zirconia compositions in and near the single-phase tetragonal region, and observed that the phase transforms martensitically to monoclinic. However, above  $\approx 4$  wt% yttria, the compositions appear within the two-phase tetragonal-cubic region, and additional types of transformations can occur. Other investigators<sup>22-24,26-29,32-36,43</sup> have cited evidence for both diffusional and displacive transformations in these systems. As the quenching or solidification rates increase, the equilibrium transformations typically observed in  $\text{Y}_2\text{O}_3$ - $\text{ZrO}_2$  alloys may be superseded by displacive transformations. As described above, our RSP alloys exhibit microstructures characteristic of both types.

Our analysis of the rapid solidification process in yttria-zirconia alloys indicates that, while the initial solidification of the melt occurs very rapidly, subsequent cooling is limited by the poor thermal conductivity of the solidified ceramic. The initial high growth rate outstrips diffusion, but once solidification has begun, the solidified material retards the removal of additional heat, and diffusion-controlled reactions become dominant in the still-hot material. The latter stages of "rapid solidification" are thus controlled by slower subsolidus processes that may alter the quenched-in microstructures and phase assemblages. Some fraction of the stabilized tetragonal  $\text{ZrO}_2$  may revert to monoclinic. When continued cooling finally inhibits diffusion, the eventual microstructures may reflect both displacive and diffusional processes. The region in which one process dominates will be a complex function of the cooling rates and the temperatures at which the respective transformations occur.



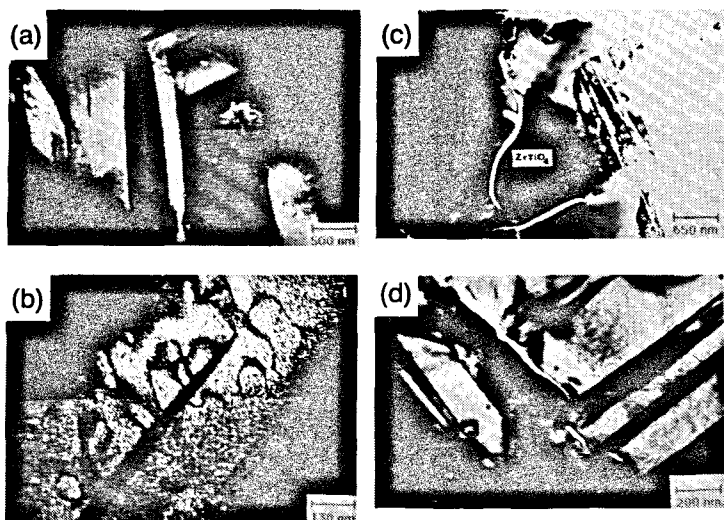


Fig. 7. Dark-field TEM of a 20 wt%  $\text{CeO}_2$  RSP alloy, (a) and (b), which show large tetragonal variants with APBs as observed in the  $\text{Y}_2\text{O}_3$  RSP alloys. A very fine modulated structure of similar scale as found in the  $\text{Y}_2\text{O}_3$  RSP alloys can be seen. However, this structure has a blocklike structure different from the tweed in Figs. 3 and 5. (c) and (d) Bright-field images of an 8 wt%  $\text{TiO}_2$  RSP alloy which shows the typical twinned monoclinic microstructure with microcracks at the intersection of the monoclinic colonies. In (c), a  $\text{ZrTiO}_4$  grain can be seen with cracks running along the grain boundary.

#### Alternative Stabilizers

The relative importance of quenching kinetics in stabilizing tetragonal  $\text{ZrO}_2$  was also evaluated for other zirconia alloy systems.  $\text{CaO}$  and  $\text{MgO}$ , commonly employed in commercial zirconia materials, could not be used, as their high vapor pressures cause significant loss of the additive during melting.  $\text{CeO}_2$  additions to zirconia have been shown to be effective in stabilizing the tetragonal phase at room temperature<sup>46–48</sup>; hence, a  $\text{ZrO}_2$  composition with 20 wt%  $\text{CeO}_2$  was quenched from the melt onto room-temperature substrates. Examination of the solid specimen revealed a solidification sequence like that of the yttria-zirconia alloy in Fig. 2, but with a slightly finer-grained layer at the melt-substrate interface. X-ray diffraction showed that the material was approximately 95 to 98% tetragonal  $\text{ZrO}_2$ . The microstructure is  $r'$  (Fig. 7(a)); tetragonal variants and APBs were visible with a fine modulated structure interspersed throughout the material. Transmission electron microscopy analyses at higher magnification (Fig. 7(b)) showed that the modulated structure was of a scale similar to the tweed structure in the yttria-zirconia alloys, although somewhat more blocky in appearance. As in the yttria-zirconia alloys, this structure may represent incipient precipitation. Overall, the microstructures suggest that both displacive and diffusional transformations have taken place.

Previous studies have indicated that  $\text{TiO}_2$  is not an effective stabilizer for tetragonal  $\text{ZrO}_2$  in conventionally processed alloys.<sup>49,50</sup> Zirconia alloyed with 8

wt%  $\text{TiO}_2$  was rapidly solidified in order to determine if the tetragonal phase could be obtained by kinetic means alone. The alloy was quenched on room-temperature substrates, as were the yttria and ceria alloys, but solidified in an entirely different manner. A uniformly fine-grained structure observed in SEM suggested that titania acted as a heterogeneous-nucleation agent during the solidification process. X-ray diffraction, SAED, and analytical electron microscopy confirmed that the  $\text{TiO}_2$  formed a monoclinic solid solution with the  $\text{ZrO}_2$ ; no tetragonal zirconia was present. The overall microstructure, depicted in Fig. 7(c), consists of colonies of monoclinic zirconia intersecting each other, and small grains of a titanate phase. The colonies consist of twins 0.2 to 0.3  $\mu\text{m}$  in average width. Where differently oriented colonies meet, strain contrast and microcracks are visible (Fig. 2(d)). Individual grains of the crystalline titanate phase,  $\text{ZrTiO}_4$  as confirmed by SAED, are present in very small amounts, with no other phases at the grain boundaries. The  $\text{ZrTiO}_4$  grains are 1 to 3  $\mu\text{m}$  in size and irregular in shape, with wavy grain boundaries, indicating that they were the last to solidify. Microcracks, arising from thermal-expansion mismatch stresses during rapid cooling, were also observed at boundaries between the monoclinic  $\text{ZrO}_2$  and the titanate phase.

These results confirm what was observed in the system yttria-zirconia: In the absence of an effective oxide stabilizer, RSP does not stabilize the high-temperature  $\text{ZrO}_2$  polymorphs.

## Summary

1. Our analyses of the system  $\text{Al}_2\text{O}_3\text{-ZrO}_2$  and the  $\text{ZrO}_2$  alloys have shown that variations in cooling rate as well as composition are possible within the rapidly solidified microstructures. Though not fully understood, these variations may be approached through analysis of the solidification process used and the thermal properties of the ceramic alloy.

2. Microstructures observed in rapidly solidified zirconia alloys indicate that both displacive (massive) and diffusional (precipitation) processes occur and compete during RSP, probably as a function of cooling rate. Diffusion-controlled subsolidus reaction may alter quenched-in phases and microstructures as the solid alloys continue to cool.

3. At rates of cooling attainable by current experiments, quenching kinetics alone do not fully stabilize the high-temperature polymorphs of  $\text{ZrO}_2$  in the absence of oxide stabilizers.

## Acknowledgments

Thanks to A. H. Heuer, T. Sakuma, G. Kalonji, J. McKittrick, M. DeGuire, T. W. Coyle, and J. S. Wallace for help and constructive discussions. Special thanks also to P. Willging and C. Verdier of NRL, for their assistance with several of the RSP experiments.

## References

- <sup>1</sup>H. Jones, "Experimental Methods in Rapid Quenching from the Melt"; pp. 1-72 in *Treatise on Materials Science and Technology, Ultrarapid Quenching of Liquid Alloys*, Vol. 20. Edited by H. Herman. Academic Press, New York, 1981.
- <sup>2</sup>A. Revcolevschi, "Rapid Solidification of Nonmetals"; pp. 73-116 in *Treatise on Materials Science and Technology, Ultrarapid Quenching of Liquid Alloys*, Vol. 20. Edited by H. Herman. Academic Press, New York, 1981.
- <sup>3</sup>P. Duwez, "Structure and Properties of Alloys Rapidly Quenched from the Liquid State," *ASM Trans.* **60**, 607-33 (1967).
- <sup>4</sup>D. Turnbull, "Metastable Structures in Metallurgy," *Met. Trans.* **12A**, 695-708 (1981).

<sup>5</sup>J. C. M. Li, "Mechanical Properties of Amorphous Metals and Alloys"; pp. 325–393 in *Treatise on Materials Science and Technology, Ultrarapid Quenching of Liquid Alloys*, Vol. 20. Edited by H. Herman. Academic Press, New York, 1981.

<sup>6</sup>C. C. Tsuei, "Electrical Properties of Liquid-Quenched Metals"; pp. 395–430 in *Treatise on Materials Science and Technology, Ultrarapid Quenching of Liquid Alloys*, Vol. 20. Edited by H. Herman. Academic Press, New York, 1981.

<sup>7</sup>K. Hashimoto and T. Masumoto, "Corrosion Behavior of Amorphous Alloys"; pp. 291–324 in *Treatise on Materials Science and Technology, Ultrarapid Quenching of Liquid Alloys*, Vol. 20. Edited by H. Herman. Academic Press, New York, 1981.

<sup>8</sup>R. L. Ashbrook (ed.), *Rapid Solidification Technology*, Source Book. American Society for Metals, Metals Park, Ohio, 1983.

<sup>9</sup>M. C. Brockway and R. R. Wills, "Rapid Solidification of Ceramics- A Technology Assessment," *Metals and Ceramics Information Center Report*, MCIC-84-49, (1984).

<sup>10</sup>A. K. Kuriakose and L. J. Beaudin, "Tetragonal Zirconia in Chilled Cast Alumina-Zirconia," *J. Can. Ceram. Soc.*, **46**, 45 (1977).

<sup>11</sup>N. Claussen, G. Lindemann, and G. Petzow, "Rapid Solidification in the  $\text{Al}_2\text{O}_3\text{-ZrO}_2$  System," *Ceram. Int.*, **9** [3] 83–86 (1983).

<sup>12</sup>G. Kalonji, J. McKittrick, and L. W. Hobbs, "Applications of Rapid Solidification Theory and Practice to  $\text{Al}_2\text{O}_3\text{-ZrO}_2$  Ceramics"; pp. 816–25 in *Advances in Ceramics* Vol. 12. Edited by N. Claussen, M. Rühle, and A. H. Heuer. The American Ceramic Society, Columbus, OH, 1984.

<sup>13</sup>B. A. Bender and R. P. Ingel, "Leaf Fossils in Ceramics"; Ceramographic Exhibit, *Am. Ceram. Soc.* **68** [8] (1985).

<sup>14</sup>B. A. Bender, R. P. Ingel, and S. C. Semken, "Dependence of Eutectic Nanostructure on Cooling Rates," Ceramographic Exhibit, *Ceram. Abs.* **65** [1–2] (1986).

<sup>15</sup>S. C. Semken, R. P. Ingel, and B. A. Bender, "Microstructures in a Rapidly Solidified Alumina-Zirconia Eutectic Alloy"; unpublished work.

<sup>16</sup>N. Claussen, "Microstructural Design of Zirconia-Toughened Ceramics (ZTC)"; pp. 325–51 in *Advances in Ceramics* Vol. 12. Edited by N. Claussen, M. Rühle, and A. H. Heuer. The American Ceramic Society, Columbus, OH, 1984.

<sup>17</sup>R. W. Rice, B. A. Bender, R. P. Ingel, and J. R. Spann, "Tougher Ceramics Using Tetragonal  $\text{ZrO}_2$  or  $\text{HfO}_2$ "; pp. 507–23 in *Ultrastructure Processing of Ceramics, Glasses and Composites*. Edited by L. L. Hench and D. R. Ulrich. Wiley & Sons, New York, 1984.

<sup>18</sup>B. A. Bender, R. P. Ingel, W. J. McDonough, and J. R. Spann, "Novel Ceramic Microstructures and Nanostructures from Advanced Processing," *Adv. Ceram. Mater.*, **1** [2] 137–44 (1986).

<sup>19</sup>W. J. Boettinger, "Growth Kinetic Limitations during Rapid Solidification"; pp. 15–31 in *Rapidly Solidified Amorphous and Crystalline Alloys*. Edited by B. H. Kear, B. C. Giessen, and M. Cohen. Elsevier, New York, 1982.

<sup>20</sup>J. H. Perepezko and W. J. Boettinger, "Use of Metastable Phase Diagrams in Rapid Solidification"; pp. 223–40 in *Rapidly Solidified Amorphous and Crystalline Alloys*. Edited by B. H. Kear, B. C. Giessen, and M. Cohen. Elsevier, New York, 1982.

<sup>21</sup>B. A. Bender, R. W. Rice, and J. R. Spann, "Precipitate Character in Laser-Melted PSZ," *J. Mater. Sci. Lett.*, **4** [11] 1331–36 (1985).

<sup>22</sup>H. G. Scott, "Phase Relationships in the Zirconia-Yttria System," *J. Mater. Sci.*, **10** [9] 1527–35 (1975).

<sup>23</sup>V. Lanteri, A. H. Heuer, and T. E. Mitchell, "Tetragonal Phase in the System  $\text{ZrO}_2\text{-Y}_2\text{O}_3$ "; pp. 118–30 in *Advances in Ceramics*, Vol. 12. Edited by N. Claussen, M. Rühle, and A. H. Heuer. The American Ceramic Society, Columbus, OH, 1984.

<sup>24</sup>V. Lanteri, R. Chaim, and A. H. Heuer, "On the Microstructures Resulting from the Diffusionless Cubic  $\rightarrow$  Tetragonal Transformation in  $\text{ZrO}_2\text{-Y}_2\text{O}_3$  Alloys," *Am. Ceram. Soc.*, **69** [10] C-258–C-261 (1986).

<sup>25</sup>J. W. Edington, *Practical Electron Microscopy in Material Science*. Van Nostrand Reinhold, London, 1976.

<sup>26</sup>B. A. Bender, "TEM Observations of APBs in PSZ Single Crystals", Ceramographic Exhibit, *Am. Ceram. Soc. Bull.*, **66** [3] 557 (1983).

<sup>27</sup>R. Chaim, M. Rühle, and A. H. Heuer, "Microstructural Evolution in a  $\text{ZrO}_2\text{-12 Weight% Y}_2\text{O}_3$  Ceramic," *J. Am. Ceram. Soc.*, **68** [8] 427–431 (1985).

<sup>28</sup>D. Michel, L. Mazerolles and M. Perez y Jorba, "Fracture of Metastable Tetragonal Zirconia Crystals," *J. Mater. Sci.*, **18** [9] 2618–28 (1983).

<sup>29</sup>A. H. Heuer and M. Rühle, "Phase Transformations in  $\text{ZrO}_2\text{-Containing Ceramics: I, The Instability of c- $\text{ZrO}_2$  and the Resulting Diffusion-Controlled Reactions$ "; pp. 1–13 in *Advances in Ceramics*, Vol. 12. Edited by N. Claussen, M. Rühle and A. H. Heuer. The American Ceramic Society, Columbus, OH, 1984.

<sup>30</sup>R. Chaim, V. Lanteri, and A. H. Heuer, "Displacive Cubic  $\rightarrow$  Tetragonal Transformation in the  $\text{ZrO}_2\text{-Y}_2\text{O}_3$  System"; unpublished work.

<sup>31</sup>W. B. Snyder and C. R. Brook, in *Proceedings of the Third Bolton Landing Conference on Ordered Alloys*, 1969. Edited by B. H. Kean, C. T. Sims, N. S. Stoloff, and J. H. Westbrook. Claitors, Baton Rouge, 1972.

- <sup>32</sup>T. Sakuma, Y. Yoshizawa, and H. Suto, "The Microstructure and Mechanical Properties of Yttria-Stabilized Zirconia Prepared by Arc-Melting," *J. Mater. Sci.*, **20** [7] 2399-2407 (1985).
- <sup>33</sup>C. A. Anderson, J. Gregg, Jr., R. C. Kuznicki, and T. K. Gupta, "Diffusionless Transformations in Zirconia Alloys"; pp. 78-85 in *Advances in Ceramics*, Vol. 12. Edited by N. Claussen, M. Rühle and A. H. Heuer. The American Ceramic Society, Columbus, OH, 1984.
- <sup>34</sup>C. A. Anderson and T. K. Gupta, "Phase Stability and Transformation Toughening in Zirconia"; pp. 184-201 in *Advances in Ceramics*, Vol. 3. Edited by A. H. Heuer and L. W. Hobbs. The American Ceramic Society, Columbus, OH, 1981.
- <sup>35</sup>T. Sakuma, Y. Yoshizawa, and H. Suto, "The Modulated Structure Formed by Isothermal Ageing in  $ZrO_2$ -5.2 Mol%  $Y_2O_3$  Alloy," *J. Mater. Sci.*, **20** [3] 1085-92 (1985).
- <sup>36</sup>T. Sakuma, Y. Yoshizawa, and H. Suto, "The Metastable Two-Phase Region in the Zirconia-Rich Part of the  $ZrO_2$ - $Y_2O_3$  System," *J. Mater. Sci.*, **21** [4] 1436-40 (1986).
- <sup>37</sup>A. H. Heuer; personal communication, 1986.
- <sup>38</sup>R. Ruh, K. S. Masdiyani, P. G. Valentine, and H. O. Bielstein, "Phase Relations in the System  $ZrO_2$ - $Y_2O_3$  at Low  $Y_2O_3$  Contents," *Am. Ceram. Soc.*, **67** [9] C-190-C-192 (1984).
- <sup>39</sup>S. Safai and H. Herman, "Plasma Sprayed Materials"; pp. 183-214 in *Treatise on Materials Science and Technology, Ultrarapid Quenching of Liquid Alloys*, Vol. 20. Edited by H. Herman. Academic Press, New York, 1981.
- <sup>40</sup>D. S. Suhr, T. E. Mitchell, and R. J. Keller, "Microstructure and Durability of Zirconia Thermal Barrier Coatings"; pp. 503-17 in *Advances in Ceramics*, Vol. 12. Edited by N. Claussen, M. Rühle, and A. H. Heuer. The American Ceramic Society, Columbus, OH, 1984.
- <sup>41</sup>L. E. Tanner, "The Ordering of  $Ni_3V$ ," *Phys. Status Solidi*, **30**, 685-701 (1968).
- <sup>42</sup>L. E. Tanner and M. F. Ashby, "On the Relief of Ordering Strains by Twinning," *Phys. Status Solidi*, **33**, 59-68 (1969).
- <sup>43</sup>N. Ishizawa, A. Saiki, T. Yagi, N. Mizutani, and M. Kato, "Twin-Related Tetragonal Variants in Yttria Partially-Stabilized Zirconia," *J. Mater. Sci. Lett.*, **4** [1] 29-30 (1985).
- <sup>44</sup>R. P. Ingel and B. A. Bender; unpublished work, U.S. Naval Research Laboratory, Washington, D. C., 20375.
- <sup>45</sup>G. Krauss and A. R. Marder, "Morphology of Martensite in Iron Alloys," *Met. Trans.*, **2**, 2343-57 (1971).
- <sup>46</sup>P. Duwez and F. Odell, "Phase Relationships in the System Zirconia-Ceria," *J. Am. Ceram. Soc.*, **33** [9] 274-83 (1950).
- <sup>47</sup>S. Roitti and V. Longo, "Investigation of Phase Equilibrium Diagrams Among Oxides by Means of Electrical Conductivity Measurements: Application of the Method to the System  $CeO_2$ - $ZrO_2$ ," *Ceramurgia Int.*, **2** [2] 97-102 (1972).
- <sup>48</sup>T. W. Coyle and W. S. Coblenz, "Phase Relations in the  $CeO_2$ - $ZrO_2$  System"; unpublished work.
- <sup>49</sup>T. Noguchi and M. Mizuno, "Phase Changes in the  $ZrO_2$ - $TiO_2$  System," *Bull. Chem. Soc. Jpn.*, **41** [12] 2895-99 (1968).
- <sup>50</sup>C. Bateman, M. Notis, and C. Lyman, "Phase Equilibria and Phase Transformations in  $ZrO_2$ - $TiO_2$  and  $ZrO_2$ - $MgO$ - $TiO_2$  Systems"; this proceedings.